IEEE Access
Multidisciplinary | Rapid Review | Open Access Journal

Received July 10, 2020, accepted July 22, 2020, date of publication July 30, 2020, date of current version August 12, 2020.

Digital Object Identifier 10.1109/ACCESS.2020.3012976

Joint Full-Duplex and Roadside Unit Selection for NOMA-Enabled V2X Communications: Ergodic Rate Performance

DINH-THUAN DO[1], (Senior Member, IEEE), MINH-SANG VAN NGUYEN[2], ANH-TU LE[2], KHALED M. RABIE[3], (Senior Member, IEEE), AND JIAYI ZHANG[4], (Member, IEEE)

[1]Wireless Communications Research Group, Faculty of Electrical & Electronics Engineering, Ton Duc Thang University, Ho Chi Minh City 700000, Vietnam
[2]Faculty of Electronics Technology, Industrial University of Ho Chi Minh City (IUH), Ho Chi Minh City 700000, Vietnam
[3]Department of Engineering, Manchester Metropolitan University, Manchester M1 5GD, U.K.
[4]School of Electronic and Information Engineering, Beijing Jiaotong University, Beijing 100044, China

Corresponding authors: Dinh-Thuan Do (dodinhthuan@tdtu.edu.vn) and Khaled M. Rabie (k.rabie@mmu.ac.uk)

ABSTRACT Vehicle-to-everything (V2X) communications are regarded as the key technology in future vehicular networks. V2X features promising benefits in providing efficient and reliable massive connections, improving traffic efficiency and safety, as well as supporting in-vehicle entertainment and other functions. Recently, non-orthogonal multiple access (NOMA) is further known as a promising solution in the fifth-generation (5G) mobile communication systems. Such NOMA has drawn much attention because of its ability to significantly improve the network throughput and lower the accessing and transmission latency to meet the quality-of-service (QoS) requirements of many 5G-enabled applications. In this respect, this paper first considers a full-duplex (FD) transmission mode together with the Roadside Unit (RSU) selection scheme in a NOMA-V2X networks since relay selection based NOMA network is introduced as technique to increase the ergodic capacity. In the considered NOMA-V2X systems, the vehicles enable device-to-device (D2D) transmission mode to permit two nearby vehicles communicate at close distances. To further robust performance, the vehicle requires relaying transmission in group of RSUs which tight connected with a cellular network. Secondly, we compare ergodic rate performance of two vehicles in specific group. Finally, we evaluate the ergodic performance by deriving the exact and closed-form expressions of ergodic rate in various scenarios. The results show that ergodic rate improvement can be achieved by increasing the number of RSUs and limiting impact of self-interference due to the FD mode.

INDEX TERMS Vehicle-to-everything, non-orthogonal multiple access, ergodic rate, device-to-device.

I. INTRODUCTION

By using a new dimension, power domain-based non-orthogonal multiple access (NOMA) is capable of supporting ultra high connectivity for foreseeable applications [1]. It is demonstrated that the NOMA is always better than the conventional orthogonal multiple access (OMA) approaches in terms of the system throughput [2]. Different from the well-known water-filling scheme, NOMA tends to allocate more power to the users with weaker channel conditions, and hence the user fairness can be guaranteed [3]. Furthermore, it has been shown that cooperative NOMA-assisted network (for example recent work reported in [4]) achieves a larger total throughput in both uplink and downlink of a wireless network compared to cooperative OMA counterpart [5]–[8]. Compared to conventional opportunistic schemes, a higher fairness is achieved by NOMA [9]. The low latency property of NOMA together with realizing a tradeoff between total throughput and fairness makes NOMA very attractive for 5G, for example a unified framework for hybrid satellite/unmanned aerial vehicle (HS-UAV) terrestrial relying NOMA is proposed in [10]. The tradeoff between throughput and fairness for a generic communication scheme has been analytical derived by [11]. Moreover, in [12] an analytical framework is proposed to derive the trade-off between performance and fairness under certain general assumptions. Such fairness feature is confirmed in NOMA. In other line of research, device-to-device (D2D) transmission is a promising technology that can alleviate traffic in core networks as well as increase mobility without rerouting data through NodeB

The associate editor coordinating the review of this manuscript and approving it for publication was Barbara Masini.

in a cellular network. In fact, D2D is expected to support proximity-based services such as social networking and file sharing. When the devices are in close vicinity, D2D communication improves the spectral and energy efficiency of cellular networks [13]. Despite the significant benefits of D2D communications in underlay mode, interference management and energy efficiency are still necessary to study as fundamental requirements [14] in keeping the interference caused by the D2D users under control, while simultaneously extending the battery lifetime of the User Equipment (UE). A D2D network employing NOMA was previously considered [15]. In particular, the authors proposed a novel concept to combine the users in a NOMA-based D2D system to groups and multiple D2D groups with respect to share sub-channels. A similar study [16] proposed the joint allocation of sub-channels and powers to maximize the sum rate of the D2D-NOMA system, while satisfying the signal to interference plus noise ratio (SINR) requirements of all D2D users in the network. The authors in [17] presented comprehensive resource allocation solution consisting of joint relay selection, user pairings, and multiple antennas design in NOMA D2D network. Motivated by these analyses and novelty from our recent work [17], [18], this study considers D2D transmission in relay selection NOMA for V2X system.

Regarding V2X networks, they are considered as one of the emerging and promising technologies to implement Internet of Things (IoT) networks. Various vehicle-based applications are served for popular objects such as passengers, vehicle traffic, drivers, and pedestrians. They enable traditional vehicles activities with more efficient and safer driving experience to drivers in their daily life. To acquire low-latency and high-reliability in various applications, V2X communications need suitable protocols to provide safety critical services for our future life [19]. For example, end-to-end latency occurs in a few milliseconds in some of delay-sensitive services [20]. Recently, by expanding the the 3rd generation partnership project (3GPP) LTE D2D communications, one can combine 3GPP Long Term Evolution (LTE)-with cellular V2X solutions. The low latency, high-reliability (LLHR) and large number of connected devices are basic requirements to employ V2X applications which is different from the LTE D2D communications. These challenges become crucial demands because high demand is required to provide multiple services in the LTE-based V2X networks where exhibit severe data congestion in dense environment [21]–[23].

To improve the spectrum efficiency and reduce the latency, NOMA is introduced as a new dimension for V2X with a capability of achieving high overloading transmission over limited resources [24]. By attempting to integrate NOMA with various practical scenarios, recent papers reported advantages of enhanced performance and satisfied LLHR requirements the to facilitate V2X networks [25]–[28]. The centralized base station (BS) and the distributed power control of the vehicles are considered in the V2X broadcasting system [25], [26]. They studied mixed centralized/distributed scheme for a new NOMA-based V2X broadcasting systems. The authors in [27] presented a D2D-enhanced V2X network, in which NOMA scheme results in increasing capacity. Based on spatial reuse among all the V2X communication groups NOMA-V2X system is facilitated with the D2D-enabled resource sharing scheme and centralized resource management. Such system model provided a significant improvement in term of network performance; however, it results in a more complicated and challenging interference scenario [27]. The authors in [28] examined the optimal power allocation issues by applying two relay-assisted NOMA transmission schemes for V2X communications. They considered half-duplex (HD) and full-duplex (FD) relaying to implement NOMA in such V2X network [28].

In other trends of V2X communications, existing works on V2X networks further confirmed benefits from NOMA [25], [29], [30]. Based on NOMA, considered systems with rate of user pair can be achieved close to the capacity region [29]. They recommended joint belief propagation (BP) decoding techniques and the graph-based practical encoding. B. Di *et al.* proposed a NOMA-based mixed centralized/distributed (NOMA-MCD) scheme to reduce the resource collision as in [25] and such system is employed for NOMA with low latency communications. In [30], the authors proposed to improve the sum rate performance in the finite signal to noise ratio (SNR) regime by introducing an optimal blind interference alignment scheme together with the coexisting of FD and HD modes. However, most of these studies relying on NOMA-V2X and FD-based V2X communications did not consider relay selection technique to improve the system performance in term of detecting signal at the vehicle, which is a challenge for finding suitable model for V2X vehicles because of limitations of design for the cellular network infrastructure. For example, the authors in [28] did not concern ergodic rate and Roadside Unit (RSU) selection as the promising method to achieve better ergodic capacity. Motivated by advantages of NOMA-assisted V2X networks, this paper proposes the method to apply RSU selection paradigm to improve performance of vehicles. In particular, we investigate the ergodic capacity in NOMA-V2X networks, where both NOMA and spatial reuse-based resource sharing for V2X communications are coexisting under the control of the BS and RSU. More specifically, the network capacity is significantly improved with the help of RSU selection scheme applied in the investigated NOMA-V2X systems, and such capacity was verified by simulation results. The main contributions of this paper are summarized as follows.

- In order to meet the QoS requirements of future 5G-enabled vehicular applications and different from the results reported in [28] and [31], this paper proposes the situation of two vehicles communicate to each other. These vehicles benefit from the NOMA technique, RSU selection scheme and D2D-enabled transmission for V2X communications is combined to form a novel communication architecture for 5G-enabled vehicular networks, namely NOMA-V2X.

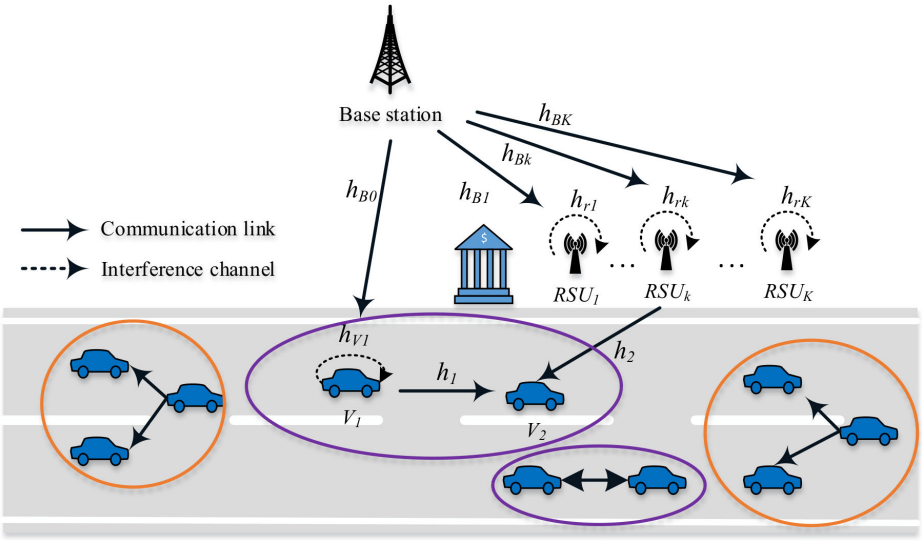

FIGURE 1. System model of NOMA-V2X relying on RSU selection.

- Depending on location of the vehicle in such networks, ergodic rate of each vehicle can be improved. We derive analytical expressions of ergodic rate for each vehicle in both exact-form and closed-form.
- Although the NOMA-V2X architecture has the potential to considerably improve the rate performance [28], extra improvement can be achieved by employing both FD and RSU selection. Furthermore, it is very challenging due to existence of the self-interference related to FD mode. Therefore, we careful examine such parameters and other significant parameters which make degraded performance in term of ergodic rate.

The remainder of this paper is organized as follows. In Section II, we present the system model of the investigated NOMA-integrated V2X scenario and analyze receiving signal to compute the SINR to further achieve corresponding ergodic rates in next section. Section III gives the detailed computations of ergodic rates for two vehicles in NOMA-V2X while OMA-V2X is presented in Section IV. In Section V, the simulation methods, details and results are considered and evaluated. We conclude key findings in Section VI.

II. SYSTEM MODEL

A. SCHEME I: NOMA-V2X

Considering a NOMA system as in Fig. 1 consisting of one BS, K RSUs acting as relaying nodes and 2 devices (V_1, V_2). We continue to consider a situation that the first vehicle receives a signal directly from the BS due to no obstruction between the BS and V_1 and such vehicle V_1 carries out its main duty as a Decode and Forward (DF) relay. After choosing the best relay among group of K RSUs ($RSU_k, k = 1, 2, \ldots, K$) and the vehicle V_2 has a chance to receive signals from the these K relays. It is more advantageous to employ FD mode at each RSU to archive higher spectrum efficiency, self-interference channel at k-th relay is denoted as h_{rk}.[1] In addition, V_2 also receives signals from V_1. However, there is no opportunity for the vehicle V_1 to obtain signals from K RSUs due to serve attenuation. To strengthen the ability of receiving better signal at the vehicle V_2, the BS intends to communicate with the second vehicle V_2 via the assistance of the near vehicle V_1. In this regard, V_1 is considered as extra relay node which operates in DF mode to forward the information to the second vehicle V_2. To enable FD communication, V_1 is equipped with one transmit antenna and one receive antenna, while the BS and V_2 are equipped with single antenna architecture. To evaluate effectiveness of FD, V_1 can still support HD mode and then it is able to switch the operation between FD and HD modes depending the demand. All wireless links in the network are assumed to be independent non-selective block Rayleigh fading and are disturbed by additive white Gaussian noise (AWGN) with mean power N_0. While $w_j, j = (1, 2, 12, r)$ are AWGN at all devices in the network are $w_j \sim CN\ (0, N_0)$. Table 1 provides remaining main parameters used in this model.

In the NOMA-V2X architecture, three main types of communication groups co-exist, i.e., the V2I group, the multi-V2V group, and the uni-V2V group. Different

[1]Regarding the self-interference cancellation scheme, active cancellation techniques are be considered in active components and achieved the knowledge of a receivers' own self-interference signal in generating a cancellation signal which can be subtracted from the received signal [32]. The methods of active mitigation techniques can be classified into three schemes including active analogue cancellation and active digital cancellation and mixed active analogue/active digital schemes. We do not want to focus on details of such schemes. In practical scenario, self-interference circuit consists of multiple components, especially the transmit signal is corrupted by impairments including non-linearity, phase and quantization noise. It is worth noting that the active cancellation method employed before the digitization of the received signal [33].

TABLE 1. Key parameters of the system model.

Symbol	Description
x_i	The information symbol to Di, $(i = 1, 2)$
x_{V1}	Loop interference signal at V_1
x_r	Loop interference signal at RSU
θ_i	The power allocation coefficient
υ	Has two mode: conversion operation between FD and HD each other
P_B	The normalized transmission powers at the BS
P_{V1}	The normalized transmission powers at V_1
P_r	The normalized transmission powers at relay
ρ	Set to P_B/N_0, where $P_B = P_{V1} = P_r$, ρ is the transmit signal-to-noise radio (SNR) and N_0 is the variance of AWGN
h_{B0}	The Rayleigh fading channel coefficients of the BS to V_1 with $h_{B0} \sim CN(0, \lambda_{hB0})$
h_{Bk}	The Rayleigh fading channel coefficients of the BS to relay with $h_{Bk} \sim CN(0, \lambda_{hBk})$, $(k = 1, \ldots, K)$
h_1	The Rayleigh fading channel coefficients of the V_1 to V_2 with $h_1 \sim CN(0, \lambda_{h1})$
h_2	The Rayleigh fading channel coefficients of the relay to V_2 with $h_2 \sim CN(0, \lambda_{h2})$
h_{V1}	The Rayleigh fading channel coefficients at V_1 with $h_{V1} \sim CN(0, \lambda_{hV1})$
h_{rk}	The Rayleigh fading channel coefficients at relay with $h_r \sim CN(0, \lambda_{hr})$

communication groups can share the spectrum resources through D2D underlaying based spatial reuse. This system model provides V2I and V2V and then further allows two vehicles to communicate with each other. In this regard, NOMA is employed in both V2I and V2V groups to increase the intra-group transmission efficiency. As a result, the introduced NOMA-V2X architecture can sufficiently exploit both the advantages of NOMA and spatial reuse of D2D in improving the spectrum efficiency.

The composed signal $x_B^{(N)}$ is transmitted from the BS to all RSU relays and related vehicle in the first phase, such signal is given as

$$x_B^{(N)} = \sqrt{\theta_1 P_B} x_1 + \sqrt{\theta_2 P_B} x_2, \tag{1}$$

where $\theta_1 + \theta_2 = 1$ and it is assumed that $\theta_1 < \theta_2$; x_1 and x_2 are signals to serve the vehicles V_1 and V_2, respectively. It is noted that x_1 and x_2 are superimposed signals to be normalized unity power signals, i.e, $E\{x_1^2\} = E\{x_2^2\} = 1$.

The received signal at V_1 in the direct link is expressed by

$$\begin{aligned} y_{B\to V1}^{(N)} &= h_{B0} x_B^{(N)} + w_1 \\ &= h_{B0}\left(\sqrt{\theta_1 P_B} x_1 + \sqrt{\theta_2 P_B} x_2\right) + h_{V1}\sqrt{\upsilon P_{V1}} x_{V1} + w_1, \end{aligned} \tag{2}$$

where $\upsilon = 1$ and $\upsilon = 0$ are indicated for the situation whether V_1 which works in FD and HD mode, respectively.

Regarding decoding order, to satisfy the requirement of NOMA, the strong signal at the vehicle V_1 must first decode the signal related to the first vehicle V_1 that has the weak signal. Such condition happens since $\theta_1 < \theta_2$. Then, once the weak device's message is detected, the vehicle V_1 is able to detect its own signal by performing a successive interference cancellation (SIC) technique. We then compute the signal-interference plus noise ratio (SINR) to detect signal x_2 at the first vehicle V_1 as [2]

$$\gamma_{BV1\leftarrow 2}^{(N)} = \frac{\theta_2 \rho |h_{B0}|^2}{\theta_1 \rho |h_{B0}|^2 + \upsilon \rho |h_{V1}|^2 + 1}. \tag{3}$$

By performing SIC, the first vehicle V_1 can detect its own signal through computing the SNR as

$$\gamma_{BV1}^{(N)} = \frac{\theta_1 \rho |h_{B0}|^2}{\upsilon \rho |h_{V1}|^2 + 1}. \tag{4}$$

The received signal at R_k is given by

$$\begin{aligned} y_{B\to Rk}^{(N)} &= h_{Bk} x_B^{(N)} + w_r \\ &= h_{Bk}\left(\sqrt{\theta_1 P_B} x_1 + \sqrt{\theta_2 P_B} x_2\right) + h_{rk}\sqrt{\upsilon P_r} x_r + w_r. \end{aligned} \tag{5}$$

The SINR of links related the RSUs to detect x_2 can be expressed as

$$\gamma_{SRk}^{(N)} = \frac{\theta_2 \rho |h_{Bk}|^2}{\theta_1 \rho |h_{Bk}|^2 + \upsilon \rho |h_{rk}|^2 + 1}. \tag{6}$$

It is noted that signal x_2 is detected at the selected RSU and then forwarded to the second vehicle V_2. We call all RSU relays having the same power P_r. In particular, the received signal can be seen at V_2, thanks to receiving from link between the RSU and V_2, as

$$y_{Rk\to V_2}^{(N)} = h_2 \sqrt{P_r} x_2 + w_2. \tag{7}$$

The corresponding SNR to detect x_2 at vehicle V_2 is given as

$$\gamma_{RkV2}^{(N)} = \rho |h_2|^2. \tag{8}$$

Regarding the D2D hop transmission, the received signal at V_2 can be achieved from link V_1 to V_2 to proceed signal x_2 as

$$y_{V1\to V2}^{(N)} = h_1 \sqrt{P_r} x_2 + w_{12}. \tag{9}$$

Next, with regard to the link from V_1 to V_2, we can determine the SNR to detect signal x_2 at V_2 as

$$\gamma_{V12}^{(N)} = \rho |h_1|^2. \tag{10}$$

The best relay node is selected by the following criterion

$$\Gamma_{k*}^{(N)} = \underbrace{\max}_{k=1\cdots K}\left(\min\left(\gamma_{SRk}^{(N)}, \gamma_{RkV2}^{(N)}\right)\right). \tag{11}$$

The instantaneous SINR at the vehicle V_2 can be written as

$$\gamma_{V2}^{(N)} = \max\left[\min\left(\gamma_{BV1\leftarrow 2}^{(N)}, \gamma_{V12}^{(N)}\right), \Gamma_{k*}^{(N)}\right]. \tag{12}$$

[2]In this paper, it is assumed that different demand of detecting signal results in ability to achieve signal x_1, x_2 at the vehicle V_1 while only x_2 need be detected at the vehicle V_2.

B. SCHEME II: OMA

This is the case when each vehicle intends to receive its own separated signal. Therefore, nodes only proceed signal related to them. The received signal at V_1 in the direct link is expressed as

$$y_{B\to V1}^{(O)} = h_{B0}\sqrt{P_B}x_1 + h_{V1}\sqrt{\upsilon P_{V1}}x_{V1} + w_1. \quad (13)$$

We first compute SNR to detect signal x_1 as below

$$\gamma_{BV1}^{(O)} = \frac{\rho|h_{B0}|^2}{\upsilon\rho|h_{V1}|^2+1}. \quad (14)$$

In a two-hop transmission side, RSU is able to receive the signal x_2 to further transmit to the second vehicle V_2. In this regard, the received signal at R_k is formulated by

$$y_{B\to Rk}^{(O)} = h_{Bk}\sqrt{P_B}x_2 + h_{rk}\sqrt{\upsilon P_r}x_r + w_r. \quad (15)$$

To detect the signal x_2 at the r_{th} relay RSU related to link the BS to relay, SNR can be written as

$$\gamma_{SRk}^{(O)} = \frac{\rho|h_{Bk}|^2}{\upsilon\rho|h_{rk}|^2+1}. \quad (16)$$

At the second vehicle V_2, the received signal can be expressed as

$$y_{Rk\to V_2}^{(O)} = h_2\sqrt{P_r}x_2 + w_2. \quad (17)$$

In the case of OMA, the SNR to detect x_2 can be computed at V_2 as

$$\gamma_{RkV2}^{(O)} = \rho|h_2|^2. \quad (18)$$

Similar as NOMA, D2D transmission can be enabled to provide the second chance for the vehicle V_2 to collect signal x_2 in the different ways. This requirement needs the help of vehicle V_1, the received signal at V_2 as receiving signal from V_1 as

$$y_{V1\to V2}^{(O)} = h_1\sqrt{P_r}x_2 + w_{12}. \quad (19)$$

Performing transmission from V_1 to V_2 with corresponding SNR as below to detect signal x_2

$$\gamma_{V12}^{(O)} = \rho|h_1|^2. \quad (20)$$

The best relay node can be obtained with similar criterion as reported in the NOMA mode. The best SNR related to this selection is given as

$$\Gamma_{k*}^{(O)} = \underbrace{\max}_{k=1\cdots K}\left(\min\left(\gamma_{SRk}^{(O)}, \gamma_{RkV2}^{(O)}\right)\right). \quad (21)$$

The instantaneous SINR at the vehicle V_2 can be written as

$$\gamma_{V2}^{(O)} = \max\left[\min\left(\gamma_{BV1\leftarrow 2}^{(O)}, \gamma_{V12}^{(O)}\right), \Gamma_{k*}^{(O)}\right]. \quad (22)$$

In the next section, the important metric should be examined to exhibit how large ergodic rates at each vehicle are.

III. ERGODIC RATE IN CASE OF NOMA

A. ERGODIC RATE FOR V_1

The main metric of ergodic rate can be computed after achieving instantaneous capacity. Such capacity depends on the obtained SINR as presented in previous section. The instantaneous capacity of V_1 in FD mode can be given by

$$C_{V1}^{(N-FD)} = \log\left(1+\gamma_{BV1}^{(N)}\right). \quad (23)$$

Proposition 1: The closed-form expression for the ergodic rate of signal at the vehicle V_1 is given as

$$C_{V1}^{(N-FD)} = \frac{\theta_1\rho\lambda_{hB0}}{\ln 2\,(\upsilon\rho\lambda_{hV1}-\theta_1\rho\lambda_{hB0})} \times\left(\exp\left(\frac{1}{\theta_1\rho\lambda_{hB0}}\right)\mathrm{Ei}\left(-\frac{1}{\theta_1\rho\lambda_{hB0}}\right) - \exp\left(\frac{1}{\upsilon\rho\lambda_{hV1}}\right)\mathrm{Ei}\left(-\frac{1}{\upsilon\rho\lambda_{hV1}}\right)\right). \quad (24)$$

It is noted that the definition of the exponential integral as $\mathrm{Ei}(x)$.

Proof: See Appendix A.

In HD mode, the closed-form expression to indicate ergodic rate for the vehicle V_1 is then computed as

$$C_{V1}^{(N-HD)} = -\frac{1}{2\ln 2}\exp\left(\frac{1}{\theta_1\rho\lambda_{hB0}}\right)\mathrm{Ei}\left(-\frac{1}{\theta_1\rho\lambda_{hB0}}\right). \quad (25)$$

B. ERGODIC RATE FOR V_2

1) ERGODIC RATE FOR V_2 RELATED TO LINK V_1-V_2

With regard to the link V_1-V_2, the received signals at V_2 come from two ways. In particular, the ergodic rate of signal x_2 at the vehicle V_2 in FD mode can be expressed as

$$C_{V2\leftarrow V1}^{(N-FD)} = \log\left(1+\min\left(\gamma_{BV1\leftarrow 2}^{(N)}, \gamma_{V12}^{(N)}\right)\right) = \frac{1}{\ln 2}\int_0^\infty \frac{1-F_\Xi(x_1)}{1+x_1}\mathrm{d}x_1, \quad (26)$$

where $\Xi = \min\left(\gamma_{BV1\leftarrow 2}^{(N)}, \gamma_{V12}^{(N)}\right)$.

Proposition 2: The exact-form to examine ergodic rate of V_2 is given as

$$C_{V2\leftarrow V1}^{(N-FD)} = \frac{1}{\ln 2}\int_0^{\frac{\theta_2}{\theta_1}} \frac{\psi_1}{(1+x_1)\,(\psi_1+x_1\upsilon\rho\lambda_{hV1})} \times\exp\left(-\xi_1 x_1\right)\mathrm{d}x_1, \quad (27)$$

where $\psi_1 = (\theta_2-x_1\theta_1)\,\rho\lambda_{hB0}$, $\xi_1 = \frac{1}{\psi_1}+\frac{1}{\rho\lambda_{h1}}$.

Proof: See Appendix B.

In HD mode, the exact-form expression of ergodic rate for V_2 is formulated by

$$C_{V2\leftarrow V1}^{(N-HD)} = \frac{1}{2\ln 2}\int_0^{\frac{\theta_2}{\theta_1}} \frac{1}{1+x_1}\exp\left(-\xi_1 x_1\right)\mathrm{d}x_1. \quad (28)$$

2) ERGODIC RATE FOR V_2 RELATED TO LINK RSU-V_2

In a NOMA-V2X system with some vehicles that are located near the RSU, the best RSU is selected to serve the second vehicle V_2. In particular, by using the definition of ergodic

rate, and such rate depends on the signal from selected RSU with index of k^*. The instantaneous ergodic rate of V_2 in this regard in FD mode can be expressed as

$$C_{V2\leftarrow R}^{(N-FD)} = \log\left(1+\Gamma_{k*}^{(N)}\right) = \frac{1}{\ln 2}\int_0^{\infty}\frac{1-F_{\Gamma_{k*}^{(N)}}(x_2)}{1+x_2}\mathrm{d}x_2. \quad (29)$$

Proposition 3: Under the help of link selected RSU-V_2 and in FD mode, the ergodic rate of V_2 can be expressed in exact form as

$$C_{V2\leftarrow R}^{(N-FD)} = \frac{1}{\ln 2}\int_0^{\frac{\theta_2}{\theta_1}}\frac{1}{1+x_2}\times\left[1-\prod_{k=1}^{K}\left(1-\frac{\psi_2}{\psi_2+x_2\upsilon\rho\lambda_{hr}}\exp\left(-\xi_2 x_2\right)\right)\right]\mathrm{d}x_2, \quad (30)$$

where $\psi_2 = (\theta_2 - x_2\theta_1)\,\rho\lambda_{hBk}$, $\xi_2 = \frac{1}{\psi_2}+\frac{1}{\rho\lambda_{h2}}$.

Proof: See Appendix C.

In HD mode, the exact-form expression of ergodic rate at V_2 is calculated by

$$C_{V2\leftarrow R}^{(N-HD)} = \frac{1}{\ln 2}\int_0^{\frac{\theta_2}{\theta_1}}\frac{1}{1+x_2}\times\left[1-\prod_{k=1}^{K}\left(1-\exp\left(-\xi_2 x_2\right)\right)\right]\mathrm{d}x_2. \quad (31)$$

3) ERGODIC RATE FOR V_2 WHEN ENABLING LINK RSU-V_2 AND LINK V_1-V_2

Similar to previous computation related to the ergodic rate, the instantaneous capacity of V_2 in FD in case of two links can be expressed as

$$C_{V2\leftarrow V1R}^{(N-FD)} = \log\left(1+\gamma_{V2}^{(N)}\right) = \frac{1}{\ln 2}\int_0^{\infty}\frac{1-F_{\gamma_{V2}^{(N)}}(x_3)}{1+x_3}\mathrm{d}x_3. \quad (32)$$

Proposition 4: The exact expression of the ergodic rate in FD for the vehicle V_2 is given as

$$C_{V2\leftarrow V1R}^{(N-FD)} = \frac{1}{\ln 2}\int_0^{\frac{\theta_2}{\theta_1}}\frac{1}{1+x_3}\mathrm{d}x_3 - \frac{1}{\ln 2}\int_0^{\frac{\theta_2}{\theta_1}}\frac{1}{1+x_3}\left[\left(1-\frac{\psi_{3a}}{\psi_{3a}+x_3\upsilon\rho\lambda_{hV1}}\exp\left(-\xi_{3a}x_3\right)\right)\times\prod_{k=1}^{K}\left(1-\frac{\psi_{3b}}{\psi_{3b}+x_3\upsilon\rho\lambda_{hr}}\exp\left(-\xi_{3b}x_3\right)\right)\right]\mathrm{d}x_3, \quad (33)$$

where $\psi_{3a} = (\theta_2 - x_3\theta_1)\,\rho\lambda_{hB0}$, $\psi_{3b} = (\theta_2 - x_3\theta_1)\,\rho\lambda_{hBk}$, $\xi_{3a} = \frac{1}{(\theta_2-x_3\theta_1)\rho\lambda_{hB0}}+\frac{1}{\rho\lambda_{h1}}$, $\xi_{3b} = \frac{1}{(\theta_2-x_3\theta_1)\rho\lambda_{hBk}}+\frac{1}{\rho\lambda_{h2}}$.

Proof: See Appendix D.

Then, the exact expression of the ergodic rate for V_2 in HD mode can be formulated as

$$C_{V2\leftarrow V1R}^{(N-HD)} = \frac{1}{\ln 2}\int_0^{\frac{\theta_2}{\theta_1}}\frac{1}{1+x_3}\mathrm{d}x_3 - \frac{1}{\ln 2}\int_0^{\frac{\theta_2}{\theta_1}}\frac{1}{1+x_3}\times\left[\left(1-\exp\left(-\xi_{3a}x_3\right)\right)\times\prod_{k=1}^{K}\left(1-\exp\left(-\xi_{3b}x_3\right)\right)\right]\mathrm{d}x_3. \quad (34)$$

IV. ERGODIC RATE IN CASE OF OMA

A. ERGODIC RATE FOR V_1

Similar to the previous case, the ergodic rate of V_1 in FD mode can be given by

$$C_{V1}^{(O-FD)} = \frac{1}{2}\log\left(1+\gamma_{BV1}^{(O)}\right) = \frac{1}{2\ln 2}\int_0^{\infty}\frac{1-F_{\gamma_{BV1}^{(O)}}(z)}{1+z}\mathrm{d}z. \quad (35)$$

Fortunately, $F_{\gamma_{BV1}^{(O)}}(z)$ can be calculated as follow

$$\begin{aligned}F_{\gamma_{BV1}^{(O)}}(z) &= \Pr\left(\gamma_{BV1}^{(O)} < z\right) = \Pr\left(|h_{B0}|^2 < \frac{z\left(\upsilon\rho|h_{V1}|^2+1\right)}{\rho}\right)\\ &= \int_0^{\infty}\exp\left(-\frac{z\upsilon\rho a+z}{\phi}\right)\frac{1}{\lambda_{hV1}}\exp\left(-\frac{a}{\lambda_{hV1}}\right)\mathrm{d}a\\ &= \frac{\phi}{z\varepsilon+\phi}\exp\left(-\frac{z}{\phi}\right), \end{aligned} \quad (36)$$

where $\phi = \rho\lambda_{hB0}$.

The closed-form expression of the ergodic rate for V_1 in FD mode is given as

$$\begin{aligned}C_{V1}^{(O-FD)} &= \frac{1}{2\ln 2}\int_0^{\infty}\frac{\lambda_{hB0}}{(1+z)\left(z\upsilon\lambda_{hV1}+\lambda_{hB0}\right)}\exp\left(-\frac{z}{\phi}\right)\mathrm{d}z\\ &= \frac{1}{2\ln 2}\int_0^{\infty}\frac{-\lambda_{hB0}}{(1+z)\,\varphi}\exp\left(-\frac{z}{\phi}\right)\mathrm{d}z\\ &\quad+\frac{1}{2\ln 2}\int_0^{\infty}\frac{\upsilon\lambda_{hB0}\lambda_{hV1}}{\left(z\upsilon\lambda_{hV1}+\lambda_{hB0}\right)\varphi}\exp\left(-\frac{z}{\phi}\right)\mathrm{d}z\\ &= \frac{\lambda_{hB0}}{2\ln 2\varphi}\left[\exp\left(\frac{1}{\phi}\right)\mathrm{Ei}\left(-\frac{1}{\phi}\right)-\exp\left(\frac{1}{\varepsilon}\right)\mathrm{Ei}\left(-\frac{1}{\varepsilon}\right)\right], \end{aligned} \quad (37)$$

where $\varphi = \upsilon\lambda_{hV1}-\lambda_{hB0}$, $\varepsilon = \upsilon\rho\lambda_{hV1}$.

In similar computation at HD mode, the closed-form expression of ergodic rate for V_1 is given as

$$C_{V1}^{(O-HD)} = -\frac{1}{4\ln 2}\exp\left(\frac{1}{\phi}\right)\mathrm{Ei}\left(-\frac{1}{\phi}\right). \quad (38)$$

B. ERGODIC RATE FOR V_2 IN OMA

1) ERGODIC RATE AT V_2 WHEN SIGNAL ACHIEVED FROM V_1-V_2

The ergodic rate of V_2 in FD, when the signal can be received from link V_1-V_2, can be expressed as

$$C_{V2\leftarrow V1}^{(O-FD)} = \frac{1}{2}\log\left(1+\min\left(\gamma_{BV1}^{(O)}, \gamma_{V12}^{(O)}\right)\right) = \frac{1}{2\ln 2}\int_0^{\infty}\frac{1-F_{\Upsilon}(z_1)}{1+z_1}\mathrm{d}z_1, \quad (39)$$

where $\Upsilon = \min\left(\gamma_{BV1}^{(O)}, \gamma_{V12}^{(O)}\right)$.

Note that $F_{\Upsilon}(z_1)$ is calculated by

$$\begin{aligned} &F_{\Upsilon}(z_1) \\ &= \Pr\left(\min\left(\gamma_{BV1}^{(O)}, \gamma_{V12}^{(O)}\right) < z_1\right) \\ &= 1-\Pr\left(\gamma_{V12}^{(O)} \geq z_1\right)\Pr\left(\gamma_{BV1}^{(O)} \geq z_1\right) \\ &= 1-\Pr\left(|h_1|^2 \geq \frac{z_1}{\rho}\right)\Pr\left(|h_{B0}|^2 \geq \frac{z_1\upsilon\rho|h_{V1}|^2+z_1}{\rho}\right) \\ &= 1-\exp\left(-\frac{z_1}{\rho\lambda_{h1}}\right)\int_0^{\infty}\exp\left(-\frac{z_1\upsilon\rho b+z_1}{\phi}\right)\frac{1}{\lambda_{hV1}} \\ &\quad\times\exp\left(-\frac{b}{\lambda_{hV1}}\right)\mathrm{d}b \\ &= 1-\frac{\lambda_{hB0}}{z_1\upsilon\lambda_{hV1}+\lambda_{hB0}}\exp\left(-\frac{z_1}{\phi}-\frac{z_1}{\rho\lambda_{h1}}\right). \end{aligned} \quad (40)$$

Plugging (40) into (39), $C_{V2\leftarrow V1}^{(O-FD)}$ can be written as in (41) shown as the top of next page, where $\Omega_1 = \frac{1}{\phi}+\frac{1}{\rho\lambda_{h1}}$.

$$\begin{aligned} &C_{V2\leftarrow R}^{(O-FD)} \\ &= \frac{1}{2\ln 2}\int_0^{\infty}\frac{1}{1+z_1}\frac{\lambda_{hB0}}{z_1\upsilon\lambda_{hV1}+\lambda_{hB0}}\exp\left(-\Omega_1 z_1\right)\mathrm{d}z_1 \\ &= \frac{1}{2\ln 2}\int_0^{\infty}\frac{-\lambda_{hB0}}{(1+z_1)\left(\upsilon\lambda_{hV1}-\lambda_{hB0}\right)}\exp\left(-\Omega_1 z_1\right)\mathrm{d}z_1 \\ &\quad+\frac{1}{2\ln 2}\int_0^{\infty}\frac{\upsilon\lambda_{hB0}\lambda_{hV1}}{\left(z_1\upsilon\lambda_{hV1}+\lambda_{hB0}\right)\left(\upsilon\lambda_{hV1}-\lambda_{hB0}\right)}\exp\left(-\Omega_1 z_1\right)\mathrm{d}z_1 \\ &= \frac{\lambda_{hB0}}{\left(\upsilon\lambda_{hV1}-\lambda_{hB0}\right)}\left[\exp\left(\Omega_1\right)\mathrm{Ei}\left(-\Omega_1\right)\right. \\ &\quad\left.-\exp\left(\frac{\lambda_{hB0}\Omega_1}{\upsilon\lambda_{hV1}}\right)\mathrm{Ei}\left(-\frac{\lambda_{hB0}\Omega_1}{\upsilon\lambda_{hV1}}\right)\right], \end{aligned} \quad (41)$$

By performing similar step, we can express the ergodic rate in HD mode for V_2 as belows

$$C_{V2\leftarrow V1}^{(O-HD)} = -\frac{1}{4\ln 2}\exp\left(\Omega_1\right)\mathrm{Ei}\left(-\Omega_1\right). \quad (42)$$

2) ERGODIC RATE FOR V_2 WHICH RECEIVES SIGNAL FORM RSU

The ergodic rate of V_2 in FD when receiving signal from relay RSU can be expressed as

$$C_{V2\leftarrow R}^{(O-FD)} = \frac{1}{2}\log\left(1+\Gamma_{k*}^{(O)}\right) = \frac{1}{2\ln 2}\int_0^{\infty}\frac{1-F_{\Gamma_{k*}^{(O)}}(z_2)}{1+z_2}\mathrm{d}z_2. \quad (43)$$

To compute (43) it need be obtained $F_{\Gamma_{k*}^{(O)}}(z_2)$ as in (44), shown at the top of the next page, where $\Omega_2 = \frac{1}{\rho\lambda_{hBk}}+\frac{1}{\rho\lambda_{h2}}$.

$$\begin{aligned} &F_{\Gamma_{k*}^{(O)}}(z_2) \\ &= \Pr\left(\underbrace{\max}_{k=1\cdots K}\left[\min\left(\gamma_{SRk}^{(O)}, \gamma_{RkV2}^{(O)}\right)\right] < z_2\right) \\ &= \prod_{k=1}^{K}\left(1-\Pr\left(\gamma_{SRk}^{(O)} \geq z_2, \gamma_{RkV2}^{(O)} \geq z_2\right)\right) \\ &= \prod_{k=1}^{K}\left(1-\Pr\left(|h_2|^2 \geq \frac{z_2}{\rho}\right)\Pr\left(|h_{Bk}|^2 \geq \frac{z_2\upsilon\rho|h_r|^2+z_2}{\rho}\right)\right) \\ &= \prod_{k=1}^{K}\left(1-\exp\left(-\frac{z_2}{\rho\lambda_{h2}}\right)\right. \\ &\quad\left.\int_0^{\infty}\exp\left(-\frac{z_2\upsilon\rho a_1+z_2}{\rho\lambda_{hBk}}\right)\frac{1}{\lambda_{hr}}\exp\left(-\frac{a_1}{\lambda_{hr}}\right)\mathrm{d}a_1\right) \\ &= \prod_{k=1}^{K}\left(1-\frac{\rho\lambda_{hBk}}{\rho\lambda_{hBk}+z_2\upsilon\rho\lambda_{hr}}\exp\left(-\Omega_2 z_2\right)\right). \end{aligned} \quad (44)$$

Finally, $C_{V2\leftarrow R}^{(O-FD)}$ can be written as

$$\begin{aligned} &C_{V2\leftarrow R}^{(O-FD)} \\ &= \frac{1}{2\ln 2}\int_0^{\infty}\frac{1}{1+z_2} \\ &\quad\times\left[1-\prod_{k=1}^{K}\left(1-\frac{\rho\lambda_{hBk}}{\rho\lambda_{hBk}+z_2\upsilon\rho\lambda_{hr}}\exp\left(-\Omega_2 z_2\right)\right)\right]\mathrm{d}z_2. \end{aligned} \quad (45)$$

The ergodic rate in HD mode for V_2 can be formulated by

$$C_{V2\leftarrow R}^{(O-HD)} = \frac{1}{4\ln 2}\int_0^{\infty}\frac{1}{1+z_2}\times\left[1-\prod_{k=1}^{K}\left(1-\exp\left(-\Omega_2 z_2\right)\right)\right]\mathrm{d}z_2. \quad (46)$$

3) ERGODIC RATE FOR V_2 WHICH RECEIVES SIGNAL FROM $RSU-V_2$ AND LINK V_1-V_2

In the OMA mode, the ergodic rate of V_2 in FD, since two links supporting to signal processing at V_2, it can be expressed as

$$C_{V2\leftarrow V1R}^{(O-FD)} = \frac{1}{2}\log\left(1+\gamma_{V2}^{(O)}\right) = \frac{1}{2\ln 2}\int_0^{\infty}\frac{1-F_{\gamma_{V2}^{(O)}}(z_3)}{1+z_3}\mathrm{d}z_3. \quad (47)$$

Similarly, $F_{\gamma_{V2}^{(O)}}(z_3)$ can be calculated as in (48), shown at the top of the next page.

$$F_{\gamma_{V2}^{(O)}}(z_3) = \Pr\left[\max\left(\min\left(\gamma_{BV1\leftarrow 2}^{(O)}, \gamma_{V12}^{(O)}\right), \Gamma_{k*}^{(O)}\right) < z_3\right]$$

$$= \Pr\left(\min\left(\gamma_{BV1\leftarrow 2}^{(O)}, \gamma_{V12}^{(O)}\right) < z_3\right) \Pr\left(\Gamma_{k*}^{(O)} < z_3\right)$$
$$= \left[1 - \frac{\lambda_{hB0}}{z_3 \upsilon \lambda_{hV1} + \lambda_{hB0}} \exp\left(-\Omega_1 z_3\right)\right] \times \prod_{k=1}^{K}\left(1 - \frac{\lambda_{hBk}}{\lambda_{hBk} + z_3 \upsilon \lambda_{hr}} \exp\left(-\Omega_2 z_3\right)\right). \quad (48)$$

Finally, the ergodic rate $C_{V2\leftarrow V1R}^{(O-FD)}$ can be given by

$$C_{V2\leftarrow V1R}^{(O-FD)} = \frac{1}{2\ln 2}\int_0^\infty \frac{1}{1+z_3}\mathrm{d}z_3 - \frac{1}{2\ln 2}\int_0^\infty \frac{1}{1+z_3} \times \left(1 - \frac{\lambda_{hB0}}{z_3 \upsilon \lambda_{hV1} + \lambda_{hB0}} \exp\left(-\Omega_1 z_3\right)\right) \times \prod_{k=1}^{K}\left(1 - \frac{\lambda_{hBk}}{\lambda_{hBk} + z_3 \upsilon \lambda_{hr}} \exp\left(-\Omega_2 z_3\right)\right)\mathrm{d}z_3. \quad (49)$$

In the HD mode, the exact-form of the ergodic rate for V_2 is given as

$$C_{V2\leftarrow V1R}^{(O-HD)} = \frac{1}{4\ln 2}\int_0^\infty \frac{1}{1+z_3}\mathrm{d}z_3 - \frac{1}{4\ln 2}\int_0^\infty \frac{1}{1+z_3} \left[1 - \exp\left(-\Omega_1 z_3\right)\right] \times \prod_{k=1}^{K}\left(1 - \exp\left(-\Omega_2 z_3\right)\right)\mathrm{d}z_3. \quad (50)$$

V. ASYMPTOTIC COMPUTATION

Due to closed-form expression is achieved for signal at the vehicle V_1, we only need consider asymptotic ergodic rate for the vehicle V_1 with ability of links occupied.

A. ASYMPTOTIC ERGODIC RATE IN NOMA CASE

1) ASYMPTOTIC ERGODIC RATE FOR V_2 RELATED TO LINK V_1 - V_2

The solution of equations, such as (27) do not admit a closed-form solution. Hence, at high SNR, Ξ can be approximated as $\Xi \triangleq \min\left(\gamma_{BV1\leftarrow 2}^{(N)}, \gamma_{V12}^{(N)}\right) \approx \min\left(\frac{\theta_2}{\theta_1}, \gamma_{V12}^{(N)}\right)$. Therefore, the approximation of $C_{V2\leftarrow V1}^{(N-FD)}$ can be computed as [35, Eq. (15)]

$$C_{V2\leftarrow V1}^{(N-FD)} \approx \int_{\frac{\theta_2}{\theta_1}}^{\infty} \log\left(1+\frac{\theta_2}{\theta_1}\right) f_{\gamma_{V12}^{(N)}}(x_1)\,\mathrm{d}x_1 + \int_0^{\frac{\theta_2}{\theta_1}} \log\left(1+x_1\right) f_{\gamma_{V12}^{(N)}}(x_1)\,\mathrm{d}x_1 \approx \frac{1}{\ln 2}\int_0^{\frac{\theta_2}{\theta_1}} \frac{1-F_{\gamma_{V12}^{(N)}}(x_1)}{1+x_1}\mathrm{d}x_1. \quad (51)$$

Applying [34, Eq. (3.352.1)] with some polynomial expansion manipulations, $C_{V2\leftarrow V1}^{(N-FD)}$ can be expressed as

$$C_{V2\leftarrow V1}^{(N-FD)} \approx \frac{1}{\ln 2}\exp\left(\frac{1}{\rho\lambda_{h1}}\right) \times \left[\mathrm{Ei}\left(-\frac{1}{\rho\lambda_{h1}}\left(\frac{\theta_2}{\theta_1}+1\right)\right) - \mathrm{Ei}\left(-\frac{1}{\rho\lambda_{h1}}\right)\right]. \quad (52)$$

2) ASYMPTOTIC ERGODIC RATE FOR V_2 RELATED TO LINK RSU - V_2

Similar to (51) and based on [34, Eq. (3.352.1)], at high SNR, $\Gamma_{k*}^{(N)} \triangleq \underbrace{\max}_{k=1\cdots K}\left(\min\left(\gamma_{SRk}^{(N)}, \gamma_{RkV2}^{(N)}\right)\right) \approx \underbrace{\max}_{k=1\cdots K}\left(\min\left(\frac{\theta_2}{\theta_1}, \gamma_{RkV2}^{(N)}\right)\right)$.

Therefore, the approximation of $C_{V2\leftarrow R}^{(N-FD)}$ can be computed as

$$C_{V2\leftarrow R}^{(N-FD)} \approx \frac{1}{\ln 2}\int_0^{\frac{\theta_2}{\theta_1}} \frac{1-F_{\gamma_{Rk*V2}^{(N)}}(x_2)}{1+x_2}\mathrm{d}x_2 \approx \sum_{k=1}^{K}\binom{K}{k}(-1)^{k-1}\frac{1}{\ln 2}\int_0^{\frac{\theta_2}{\theta_1}} \frac{1}{1+x_2}\exp\left(-\frac{kx_2}{\rho\lambda_{h2}}\right)\mathrm{d}x_2 \approx \sum_{k=1}^{K}\binom{K}{k}(-1)^{k-1}\frac{\exp\left(\frac{k}{\rho\lambda_{h2}}\right)}{\ln 2} \times \left[\mathrm{Ei}\left(-\frac{k}{\rho\lambda_{h2}}\left(\frac{\theta_2}{\theta_1}+1\right)\right) - \mathrm{Ei}\left(-\frac{k}{\rho\lambda_{h2}}\right)\right]. \quad (53)$$

3) ASYMPTOTIC ERGODIC RATE FOR V_2 WHEN ENABLING LINK RSU-V_2 AND LINK V_1-V_2

Similar to (51) and (53) and based on [34, Eq. (3.352.1)], at high SNR, $\gamma_{V2}^{(N)} = \max\left[\min\left(\gamma_{BV1\leftarrow 2}^{(N)}, \gamma_{V12}^{(N)}\right), \Gamma_{k*}^{(N)}\right] \approx \max\left[\min\left(\frac{\theta_2}{\theta_1}, \gamma_{V12}^{(N)}\right), \underbrace{\max}_{k=1\cdots K}\left[\min\left(\frac{\theta_2}{\theta_1}, \gamma_{RkV2}^{(N)}\right)\right]\right]$.

Therefore, the approximation of $C_{V2\leftarrow V1R}^{(N-FD)}$ can be expressed as

$$C_{V2\leftarrow V1R}^{(N-FD)} \approx \frac{1}{\ln 2}\int_0^{\frac{\theta_2}{\theta_1}} \frac{1-F_{\gamma_{V2}^{(N)}}(x_2)}{1+x_3}\mathrm{d}x_3 \approx \sum_{k=1}^{K}\binom{K}{k}(-1)^{k-1}\frac{1}{\ln 2} \times \int_0^{\frac{\theta_2}{\theta_1}} \frac{1}{1+x_3}\exp\left(-\left(\frac{k}{\rho\lambda_{h2}}+\frac{1}{\rho\lambda_{h1}}\right)x_3\right)\mathrm{d}x_3 \approx \sum_{k=1}^{K}\binom{K}{k}(-1)^{k-1}\frac{\exp\left(\frac{k}{\rho\lambda_{h2}}+\frac{1}{\rho\lambda_{h1}}\right)}{\ln 2} \times \left[\mathrm{Ei}\left(-\left(\frac{k}{\rho\lambda_{h2}}+\frac{1}{\rho\lambda_{h1}}\right)\left(\frac{\theta_2}{\theta_1}+1\right)\right) - \mathrm{Ei}\left(-\left(\frac{k}{\rho\lambda_{h2}}+\frac{1}{\rho\lambda_{h1}}\right)\right)\right]. \quad (54)$$

B. ASYMPTOTIC ERGODIC RATE IN OMA CASE

1) ASYMPTOTIC ERGODIC RATE FOR V_2 WHICH RECEIVES SIGNAL THROUGH RSU

Similar to (53) and based on [34, Eq. (3.352.4)], at high SNR, the approximation of $C_{V2\leftarrow R}^{(O-FD)}$ can be

written as

$$C_{V2\leftarrow R}^{(O-FD)} \approx \frac{1}{2\ln 2}\int_0^{\infty}\frac{1-F_{\Gamma_{k*}^{(O)}}(z_2)}{1+z_2}\mathrm{d}z_2 \approx \sum_{k=1}^{K}\binom{K}{k}(-1)^{k-1}\frac{1}{2\ln 2}\int_0^{\infty}\frac{1}{1+z_2}\exp\left(-\frac{kz_2}{\rho\lambda_{h2}}\right)\mathrm{d}z_2 \approx \sum_{k=1}^{K}\binom{K}{k}(-1)^{k-1}\frac{-\exp\left(\frac{k}{\rho\lambda_{h2}}\right)}{2\ln 2}\mathrm{Ei}\left(-\frac{k}{\rho\lambda_{h2}}\right). \quad (55)$$

2) ASYMPTOTIC ERGODIC RATE FOR V_2 WHICH RECEIVES SIGNAL FROM $RSU-V_2$ AND LINK V_1-V_2

Similar to (54) and based on [34, Eq. (3.352.4)]. Hence, at high SNR, the approximation of $C_{V2\leftarrow V1R}^{(O-FD)}$ can be given as

$$C_{V2\leftarrow V1R}^{(O-FD)} \approx \frac{1}{2\ln 2}\int_0^{\infty}\frac{1-F_{\gamma_{V2}^{(O)}}(x_2)}{1+z_3}\mathrm{d}z_3 \approx \sum_{k=1}^{K}\binom{K}{k}(-1)^{k-1}\frac{1}{2\ln 2}\times\int_0^{\infty}\frac{1}{1+z_3}\exp\left(-\left(\frac{k}{\rho\lambda_{h2}}+\frac{1}{\rho\lambda_{h1}}\right)z_3\right)\mathrm{d}z_3 \approx \sum_{k=1}^{K}\binom{K}{k}(-1)^{k-1}\frac{-\exp\left(\frac{k}{\rho\lambda_{h2}}+\frac{1}{\rho\lambda_{h1}}\right)}{2\ln 2}\times\mathrm{Ei}\left(-\left(\frac{k}{\rho\lambda_{h2}}+\frac{1}{\rho\lambda_{h1}}\right)\right). \quad (56)$$

VI. NUMERICAL RESULTS

In this section, the ergodic performance of the considered system is evaluated by numerical and analytical simulation. In particular, we set the power allocation factors as $\theta_1 = 0.3$, $\theta_2 = 0.7$, the main channel gains are $\lambda_{hB1} = 5$, the self-interference channel gains are $\lambda_{hBk} = \lambda_{h1} = \lambda_{h2} = 1$ and $\lambda_{hV1} = \lambda_{hr} = 0.01$, except for specific cases.

Fig. 2 depicts the ergodic capacity comparison of the NOMA-V2X system in HD/FD transmission modes with two values of $\lambda_{hB1} = 5$ and 10. It is observed that the system performance of such networks employing NOMA in FD is superior to remaining cases. A bigger gap on performance of system can be observed as comparing HD OMA case and HD NOMA case. Additionally, a stronger channel h_{B0} contributes to better ergodic rate. It is confirmed that the ergodic capacity for the vehicle V_1 increase as SNR changes form -20 (dB) to 40 (dB). It is also indicated that there is a tight matching between the simulation and analytical results for these ergodic rate performance.

The ergodic rates under impact of channel gain can be observed as in Fig. 3. It is clear that FD mode in NOMA-V2X system occurs saturation situation of ergodic rate at high SNR. Particularly, when SNR is greater than 30 (dB), there exists the upper bound of the ergodic rate. It is intuitively seen that higher levels of self-interference λ_{hV1} at the vehicle

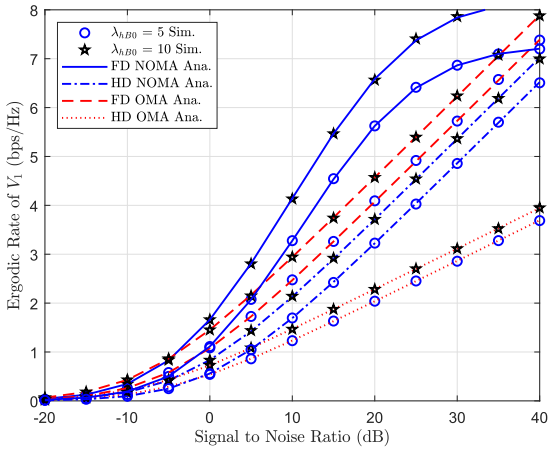

FIGURE 2. The ergodic rate of V_1 versus transmit SNR with different values of λ_{hB1}.

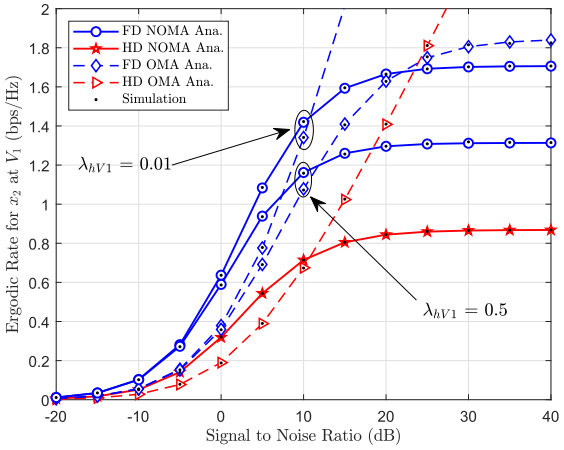

FIGURE 3. The ergodic rate of V_2 using V_1-V_2 link versus transmit SNR with different values of λ_{hV1}.

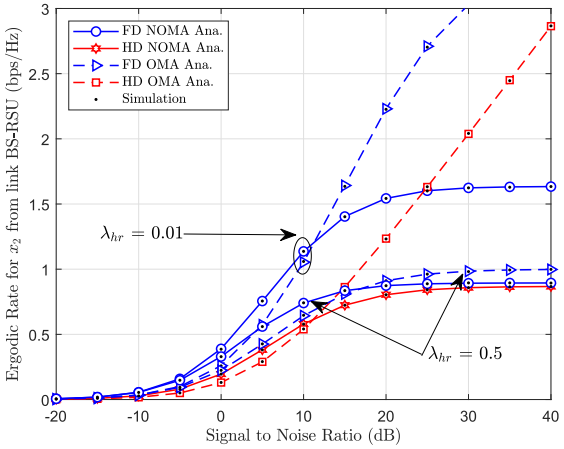

FIGURE 4. The ergodic rate of V_2 using BS-RSU link versus transmit SNR with different values of λ_{hr}.

V_1 results in a worse ergodic rate. Interestingly, such systems exhibit better ergodic performance at HD/FD in case of the OMA scheme. It is further confirmed the saturate situation

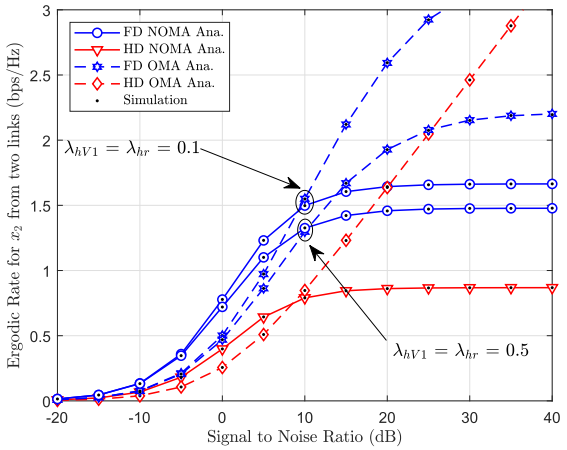

FIGURE 5. The ergodic rate at V_2 using two links versus transmit SNR with different values of λ_{hV1} and λ_{hr}.

happens at the high SNR regime due to the detrimental effect of residual self-interference at the vehicle V_1. More importantly, while the ergodic capacity can be improved by increasing the level of SNR, it can be further enhanced with lower level of self-interference λ_{hV1}. By selecting the mode OMA or NOMA, it is apparent that the ergodic rate performance gap in whole range of SNR. This agrees with the results obtained in Fig. 2 for the ergodic rate. In addition, it can be achieved the advantage of such systems as combining benefits of NOMA and FD-enabled V_1 at low region of SNR.

Considering the ergodic rate performance at the vehicle V_2 as enabling two links as in Fig. 5, the NOMA-V2X system at HD mode has the worst performance. Furthermore, lower level of self-interference at both RSU and vehicle V_1 implies better ergodic rate and such trend is as similar to the previous figures.

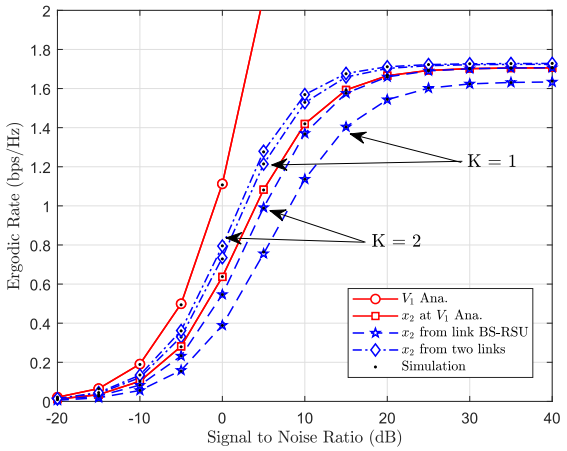

FIGURE 6. The ergodic rate versus transmit SNR with different values of K.

Fig. 6 illustrates the ergodic rate versus the transmit SNR, as well as a comparison the ergodic rate performance of the vehicle V_2 via three cases: (1) signal at V_2 comes from V_1; (2) signal at V_2 comes from relay RSU; (3) signal at V_2 comes

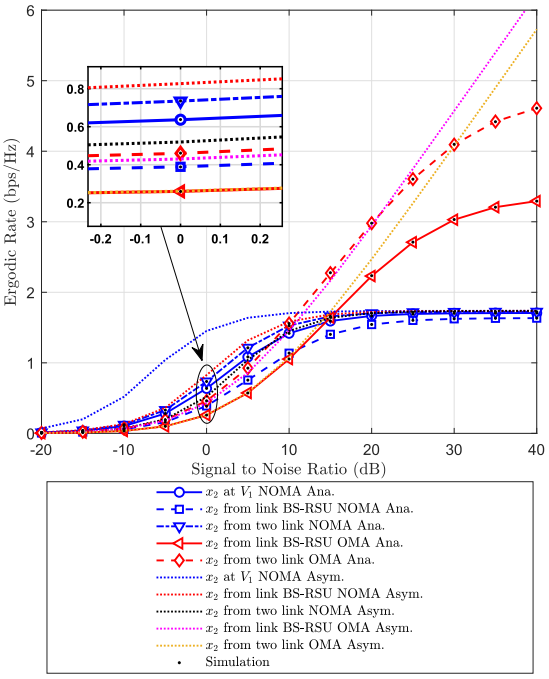

FIGURE 7. The ergodic rate comparison.

from both relay RSU and V_1. It can be observed that the best case is the ergodic rate of V_1 while the ergodic rate at V_2 can be improved slightly as enabling signal from link RSU-V_2 and link V_1−V_2 and these improved ergodic rates occur in the case of $K = 2$. This situation can be justified by the fact that more chances to receive better signal as equipping more number of RSU and more links connects to V_2.

In Fig. 7, it is confirmed that the ergodic rate of considered system meets saturation situation at high SNR. At each link, separating the ergodic capacity performance can be observed only low region of SNR.

VII. CONCLUSION

This paper investigated the ergodic rate performance of various cases of NOMA-V2X system with two vehicles which benefit from FD mode and RSU selection scheme. More chances to achieve better signal as more links are connected to the dedicated vehicle. In particular, this paper derived exact analytical expressions for the ergodic rate of each vehicle. With the aim of ergodic rate improvement, more RSUs are selected and FD is enabled. In addition, Monte Carlo simulations were provided to validate the accuracy of our formulas. Numerical results showed that the ergodic rate of NOMA-V2X can be enhanced thanks to employing FD and RSU selection mode.

APPENDIX A
PROOF OF PROPOSITION 1

From (23), it can calculated as follows

$$C_{V1}^{(N-FD)} = \frac{1}{\ln 2}\int_0^{\infty} \frac{1-F_{\gamma_{BV1}^{(N)}}(x)}{1+x}\mathrm{d}x. \qquad (A.1)$$

It is noted that $F_{\gamma_{BV1}^{(N)}}(x)$ can be further calculated as

$$\begin{aligned} F_{\gamma_{BV1}^{(N)}}(x) &= \Pr\left(\frac{\theta_1\rho|h_{B0}|^2}{\upsilon\rho|h_{V1}|^2+1} < x\right) \\ &= 1-\int_0^{\infty} \exp\left(-\frac{x\upsilon\rho y+x}{\theta_1\rho\lambda_{hB0}}\right)\frac{1}{\lambda_{hV1}}\exp\left(-\frac{y}{\lambda_{hV1}}\right)\mathrm{d}y \\ &= 1-\frac{\theta_1\rho\lambda_{hB0}}{\theta_1\rho\lambda_{hB0}+x\upsilon\rho\lambda_{hV1}}\exp\left(-\frac{x}{\theta_1\rho\lambda_{hB0}}\right). \end{aligned} \tag{A.2}$$

Plugging (A.2) into (A.1), it can calculated as ergodic rate as in the bottom of the page (A.3).

Related to (A.3), based on [34, Eq. (3.352.4)] and applying some polynomial expansion manipulations, β_1 and β_2 are given by

$$\beta_1 = \frac{\theta_1\rho\lambda_{hB0}}{(\upsilon\rho\lambda_{hV1}-\theta_1\rho\lambda_{hB0})} \times \exp\left(\frac{1}{\theta_1\rho\lambda_{hB0}}\right)\mathrm{Ei}\left(-\frac{1}{\theta_1\rho\lambda_{hB0}}\right), \tag{A.4}$$

and

$$\beta_2 = -\frac{\theta_1\rho\lambda_{hB0}}{(\upsilon\rho\lambda_{hV1}-\theta_1\rho\lambda_{hB0})} \times \exp\left(\frac{1}{\upsilon\rho\lambda_{hV1}}\right)\mathrm{Ei}\left(-\frac{1}{\upsilon\rho\lambda_{hV1}}\right). \tag{A.5}$$

Substituting (A.4) and (A.5) into (A.3), we can obtain (24). The proof is completed.

APPENDIX B
PROOF OF PROPOSITION 2

$F_{\Xi}(x_1)$ is calculated as follow

$$\begin{aligned} F_{\Xi}(x_1) &= \Pr\left(\min\left(\gamma_{BV1\leftarrow 2}^{(N)}, \gamma_{V12}^{(N)}\right) < x_1\right) \\ &= 1-\Pr\left(\gamma_{BV1\leftarrow 2}^{(N)} \geq x_1\right)\Pr\left(\gamma_{V12}^{(N)} \geq x_1\right) \\ &= 1-\Pr\left(|h_{B0}|^2 \geq \frac{x_1\upsilon\rho|h_{V1}|^2+x_1}{(\theta_2-x_1\theta_1)\rho}\right)\Pr\left(|h_1|^2 \geq \frac{x_1}{\rho}\right) \\ &= 1-\underbrace{\Pr\left(|h_{B0}|^2 \geq \frac{x_1\upsilon\rho|h_{V1}|^2+x_1}{(\theta_2-x_1\theta_1)\rho}\right)}_{\Phi} \times \exp\left(-\frac{x_1}{\rho\lambda_{h1}}\right). \end{aligned}$$

With $x_1 < \frac{\theta_2}{\theta_1}$, it can be obtained Φ as

$$\begin{aligned} \Phi &= \frac{1}{\lambda_{hV1}}\int_0^{\infty}\exp\left(-\frac{y_1}{\lambda_{hV1}}\right)\exp\left(-\frac{x_1\upsilon\rho y_1+x_1}{\psi_1}\right)\mathrm{d}y_1 \\ &= \frac{\psi_1}{\psi_1+x_1\upsilon\rho\lambda_{hV1}}\exp\left(-\frac{x_1}{\psi_1}\right). \end{aligned} \tag{B.2}$$

Substituting (B.1) and (B.2) into (26), then it results in (27). It is end of the proof.

APPENDIX C
PROOF OF PROPOSITION 3

$F_{\Gamma_{k*}^{(N)}}(x_2)$ is calculated as in (C.1) at the top of the next page.

With $x_2 < \frac{\theta_2}{\theta_1}$, it can be achieved δ as

$$\begin{aligned} \delta &= \frac{1}{\lambda_{h_{rk}}}\int_0^{\infty}\exp\left(-\frac{y_2}{\lambda_{hr}}-\frac{x_2\upsilon\rho y_2+x_2}{\psi_2}\right)\mathrm{d}y_2 \\ &= \frac{\psi_2}{\psi_2+x_2\upsilon\rho\lambda_{hr}}\exp\left(-\frac{x_2}{\psi_2}\right). \end{aligned} \tag{C.2}$$

Substituting (C.1) and (C.2) into (29), it can be shown as result in (30).

It completes the proof.

APPENDIX D
PROOF OF PROPOSITION 4

At the top of next page, it can be achieved $F_{\gamma_{V2}^{(N)}}(x_3)$ as (D.1)

$$\begin{aligned} F_{\gamma_{V2}^{(N)}}(x_3) &= \Pr\left(\max\left[\min\left(\gamma_{BV1\leftarrow 2}^{(N)}, \gamma_{V12}^{(N)}\right), \Gamma_{k*}^{(N)}\right] < x_3\right) \\ &= \underbrace{\Pr\left(\min\left(\gamma_{BV1\leftarrow 2}^{(N)}, \gamma_{V12}^{(N)}\right) < x_3\right)}_{\chi_1} \times \underbrace{\Pr\left(\Gamma_{k*}^{(N)} < x_3\right)}_{\chi_2}. \end{aligned} \tag{D.1}$$

Similarly, $F_{\Xi}(x_1)$, χ_1 can be formulated as

$$\begin{aligned} \chi_1 &= \Pr\left(\min\left(\gamma_{BV1\leftarrow 2}^{(N)}, \gamma_{V12}^{(N)}\right) < x_3\right) \\ &= 1-\frac{\psi_{3a}}{\psi_{3a}+x_1\upsilon\rho\lambda_{hV1}}\exp\left(-\xi_{3a}x_3\right). \end{aligned} \tag{D.2}$$

$$\begin{aligned} C_{V1}^{(N-FD)} &= \frac{1}{\ln 2}\int_0^{\infty}\frac{\theta_1\rho\lambda_{hB0}}{(1+x)\,(\theta_1\rho\lambda_{hB0}+x\upsilon\rho\lambda_{hV1})}\exp\left(-\frac{x}{\theta_1\rho\lambda_{hB0}}\right)\mathrm{d}x \\ &= \frac{1}{\ln 2}\underbrace{\int_0^{\infty}\frac{-\theta_1\rho\lambda_{hB0}}{(1+x)\,(\upsilon\rho\lambda_{hV1}-\theta_1\rho\lambda_{hB0})}\exp\left(-\frac{x}{\theta_1\rho\lambda_{hB0}}\right)\mathrm{d}x}_{\beta_1} \\ &\quad + \frac{1}{\ln 2}\underbrace{\int_0^{\infty}\frac{\theta_1\rho\lambda_{hB0}\upsilon\rho\lambda_{hV1}}{(\theta_1\rho\lambda_{hB0}+x\upsilon\rho\lambda_{hV1})\,(\upsilon\rho\lambda_{hV1}-\theta_1\rho\lambda_{hB0})}\exp\left(-\frac{x}{\theta_1\rho\lambda_{hB0}}\right)\mathrm{d}x}_{\beta_2}. \end{aligned} \tag{A.3}$$

$$
\begin{aligned}
F_{\Gamma_{k*}^{(N)}}(x_2) &= \Pr\left(\underbrace{\max_{k=1\cdots K}}\left[\min\left(\gamma_{SRk}^{(N)}, \gamma_{RkV2}^{(N)}\right)\right] < x_2\right) \\
&= \prod_{k=1}^{K}\left(1-\Pr\left(\gamma_{SRk}^{(N)} \geq x_2, \gamma_{RkV2}^{(N)} \geq x_2\right)\right) \\
&= \prod_{k=1}^{K}\left(1-\Pr\left(|h_{Bk}|^2 \geq \frac{x_2\upsilon\rho|h_{rk}|^2 + x_2}{(\theta_2 - x_2\theta_1)\,\rho}\right)\Pr\left(|h_2|^2 \geq \frac{x_2}{\rho}\right)\right) \\
&= \prod_{k=1}^{K}\left(\underbrace{1-\Pr\left(|h_{Bk}|^2 \geq \frac{x_2\upsilon\rho|h_{rk}|^2 + x_2}{(\theta_2 - x_2\theta_1)\,\rho}\right)}_{\delta} \times \exp\left(-\frac{x_2}{\rho\lambda_{h2}}\right)\right).
\end{aligned} \tag{C.1}
$$

Similarly $F_{\Gamma_{k*}^{(N)}}(x_2)$, χ_2 can be expressed as

$$
\begin{aligned}
\chi_2 &= \Pr\left(\Gamma_{k*}^{(N)} < x_3\right) \\
&= \prod_{k=1}^{K}\left(1-\frac{\psi_{3b}}{\psi_{3b}+x_2\upsilon\rho\lambda_{hr}}\exp\left(-\xi_{3b}x_3\right)\right).
\end{aligned} \tag{D.3}
$$

Substituting (D.1), (D.2) and (D.3) into (32), result is finalized as (33).

It is end of the proof.

REFERENCES

[1] Y. Liu, Z. Qin, M. Elkashlan, Z. Ding, A. Nallanathan, and L. Hanzo, "Nonorthogonal multiple access for 5G and beyond," *Proc. IEEE*, vol. 105, no. 12, pp. 2347–2381, Dec. 2017.

[2] K. M. Rabie and B. Adebisi, "Enhanced Amplify-and-Forward relaying in non-Gaussian PLC networks," *IEEE Access*, vol. 5, pp. 4087–4094, 2017.

[3] K. M. Rabie, B. Adebisi, E. H. G. Yousif, H. Gacanin, and A. M. Tonello, "A comparison between orthogonal and non-orthogonal multiple access in cooperative relaying power line communication systems," *IEEE Access*, vol. 5, pp. 10118–10129, 2017.

[4] D.-T. Do and A.-T. Le, "NOMA based cognitive relaying: Transceiver hardware impairments, relay selection policies and outage performance comparison," *Comput. Commun.*, vol. 146, pp. 144–154, Oct. 2019.

[5] D. T. Do, H. S. Nguyen, M. Voznak, and T. S. Nguyen, "Wireless powered relaying networks under imperfect channel state information: System performance and optimal policy for instantaneous rate," *Radioengineering*, vol. 26, no. 3, pp. 869–877, Sep. 2017.

[6] D.-T. Do, "Optimal throughput under time power switching based relaying protocol in energy harvesting cooperative networks," *Wireless Pers. Commun.*, vol. 87, no. 2, pp. 551–564, 2016.

[7] D.-T. Do, "Power switching protocol for two-way relaying network under hardware impairments," *Radioengineering*, vol. 24, no. 3, pp. 765–771, Sep. 2015.

[8] H.-S. Nguyen, A.-H. Bui, D.-T. Do, and M. Voznak, "Imperfect channel state information of AF and DF energy harvesting cooperative networks," *China Commun.*, vol. 13, no. 10, pp. 11–19, Oct. 2016.

[9] S. Timotheou and I. Krikidis, "Fairness for non-orthogonal multiple access in 5G systems," *IEEE Signal Process. Lett.*, vol. 22, no. 10, pp. 1647–1651, Oct. 2015.

[10] X. Li, Q. Wang, H. Peng, H. Zhang, D.-T. Do, K. M. Rabie, R. Kharel, and C. C. Cavalcante, "A unified framework for HS-UAV NOMA networks: Performance analysis and location optimization," *IEEE Access*, vol. 8, pp. 13329–13340, 2020.

[11] F. Zabini, A. Bazzi, and B. M. Masini, "Throughput versus fairness tradeoff analysis," in *Proc. IEEE Int. Conf. Commun. (ICC)*, Jun. 2013, pp. 5131–5136.

[12] F. Zabini, A. Bazzi, B. M. Masini, and R. Verdone, "Optimal performance versus fairness tradeoff for resource allocation in wireless systems," *IEEE Trans. Wireless Commun.*, vol. 16, no. 4, pp. 2587–2600, Apr. 2017.

[13] X. Lin, J. Andrews, A. Ghosh, and R. Ratasuk, "An overview of 3GPP device-to-device proximity services," *IEEE Commun. Mag.*, vol. 52, no. 4, pp. 40–48, Apr. 2014.

[14] P. Mach, Z. Becvar, and T. Vanek, "In-band Device-to-Device communication in OFDMA cellular networks: A survey and challenges," *IEEE Commun. Surveys Tuts.*, vol. 17, no. 4, pp. 1885–1922, Jun. 2015.

[15] J. Zhao, Y. Liu, K. K. Chai, Y. Chen, M. Elkashlan, and J. Alonso-Zarate, "NOMA-based D2D communications: Towards 5G," in *Proc. IEEE Global Commun. Conf. (GLOBECOM)*, Dec. 2016, pp. 1–6.

[16] J. Zhao, Y. Liu, K. K. Chai, Y. Chen, and M. Elkashlan, "Joint subchannel and power allocation for NOMA enhanced D2D communications," *IEEE Trans. Commun.*, vol. 65, no. 11, pp. 5081–5094, Nov. 2017.

[17] H.-P. Dang, M.-S. Van Nguyen, D.-T. Do, H.-L. Pham, B. Selim, and G. Kaddoum, "Joint relay selection, full-duplex and Device-to-Device transmission in wireless powered NOMA networks," *IEEE Access*, vol. 8, pp. 82442–82460, 2020.

[18] T.-L. Nguyen and D.-T. Do, "Power allocation schemes for wireless powered NOMA systems with imperfect CSI: An application in multiple antenna–based relay," *Int. J. Commun. Syst.*, vol. 31, no. 15, p. e3789, Oct. 2018.

[19] G. Karagiannis, O. Altintas, E. Ekici, G. Heijenk, B. Jarupan, K. Lin, and T. Weil, "Vehicular networking: A survey and tutorial on requirements, architectures, challenges, standards and solutions," *IEEE Commun. Surveys Tuts.*, vol. 13, no. 4, pp. 584–616, Sep. 2011.

[20] H. Yang, K. Zheng, K. Zhang, J. Mei, and Y. Qian, "Ultra-reliable and low-latency communications for connected vehicles: Challenges and solutions," 2017, *arXiv:1712.00537*. [Online]. Available: http://arxiv.org/abs/1712.00537

[21] S.-H. Sun, J.-L. Hu, Y. Peng, X.-M. Pan, L. Zhao, and J.-Y. Fang, "Support for vehicle-to-everything services based on LTE," *IEEE Wireless Commun.*, vol. 23, no. 3, pp. 4–8, Jun. 2016.

[22] S. Chen, J. Hu, Y. Shi, and L. Zhao, "Technologies, standards and applications of LTE-V2X for vehicular networks," *Telecommun. Sci.*, vol. 34, no. 4, pp. 1–11, Apr. 2018.

[23] T. Soni, A. R. Ali, K. Ganesan, and M. Schellmann, "Adaptive numerology—A solution to address the demanding QoS in 5G-V2X," in *Proc. IEEE Wireless Commun. Netw. Conf. (WCNC)*, Barcelona, Spain, Apr. 2018, pp. 1–6.

[24] B. Di, L. Song, Y. Li, and Z. Han, "V2X meets NOMA: Non-orthogonal multiple access for 5G-enabled vehicular networks," *IEEE Wireless Commun.*, vol. 24, no. 6, pp. 14–21, Dec. 2017.

[25] B. Di, L. Song, Y. Li, and G. Y. Li, "Non-orthogonal multiple access for high-reliable and low-latency V2X communications in 5G systems," *IEEE J. Sel. Areas Commun.*, vol. 35, no. 10, pp. 2383–2397, Oct. 2017.

[26] B. Di, L. Song, Y. Li, and G. Y. Li, "NOMA-based low-latency and high-reliable broadcast communications for 5G V2X services," in *Proc. IEEE GLOBECOM*, vol. 17. Singapore, Dec. 2017, pp. 1–6.

[27] B. Wang, R. Zhang, C. Chen, X. Cheng, L. Yang, and Y. Jin, "Interference hypergraph-based 3D matching resource allocation protocol for NOMA-V2X networks," *IEEE Access*, vol. 7, pp. 90789–90800, 2019.
[28] G. Liu, Z. Wang, J. Hu, Z. Ding, and P. Fan, "Cooperative NOMA Broadcasting/Multicasting for low-latency and high-reliability 5G cellular V2X communications," *IEEE Internet Things J.*, vol. 6, no. 5, pp. 7828–7838, Oct. 2019.
[29] B. W. Khoueiry and M. R. Soleymani, "An efficient NOMA V2X communication scheme in the Internet of vehicles," in *Proc. IEEE 85th Veh. Technol. Conf. (VTC Spring)*, Jun. 2017, pp. 1–7.
[30] M. Yang, S.-W. Jeon, and D. K. Kim, "Interference management for in-band full-duplex vehicular access networks," *IEEE Trans. Veh. Technol.*, vol. 67, no. 2, pp. 1820–1824, Feb. 2018.
[31] D. Zhang, Y. Liu, L. Dai, A. K. Bashir, A. Nallanathan, and B. Shim, "Performance analysis of FD-NOMA-Based decentralized V2X systems," *IEEE Trans. Commun.*, vol. 67, no. 7, pp. 5024–5036, Jul. 2019.
[32] A. Sahai, G. Patel, C. Dick, and A. Sabharwal, "Understanding the impact of phase noise on active cancellation in wireless full-duplex," in *Proc. Conf. Rec. 46th Asilomar Conf. Signals, Syst. Comput. (ASILOMAR)*, Nov. 2012, pp. 29–33.
[33] A. Sahai, G. Patel, C. Dick, and A. Sabharwal, "On the impact of phase noise on active cancelation in wireless full-duplex," *IEEE Trans. Veh. Technol.*, vol. 62, no. 9, pp. 4494–4510, Nov. 2013.
[34] I. S. Gradshteyn and I. M. Ryzhik, *Table of Integrals, Series and Products*, 6th ed. New York, NY, USA: Academic, 2000.
[35] J.-B. Kim and I.-H. Lee, "Non-orthogonal multiple access in coordinated direct and relay transmission," *IEEE Commun. Lett.*, vol. 19, no. 11, pp. 2037–2040, Nov. 2015.

DINH-THUAN DO (Senior Member, IEEE) received the B.S., M.Eng., and Ph.D. degrees in communications engineering from Vietnam National University (VNU-HCM), in 2003, 2007, and 2013, respectively.

He was a visiting Ph.D. student with the Communications Engineering Institute, National Tsing Hua University, Taiwan, from 2009 to 2010. Prior to joining Ton Duc Thang University, he was a Senior Engineer with the VinaPhone Mobile Network, from 2003 to 2009. He has published over 65 SCI/SCIE journal articles and one sole author book. His research interests include signal processing in wireless communications networks, cooperative communications, non-orthogonal multiple access, full-duplex transmission, and energy harvesting. He was a recipient of the Golden Globe Award from the Vietnam Ministry of Science and Technology (Top Ten Excellent Young Scientists Nationwide), in 2015. He has been serving as an Associate Editor for six journals, in which main journals are the *EURASIP Journal on Wireless Communications and Networking*, *Computer Communications* (Elsevier), and the *KSII Transactions on Internet and Information Systems*.

MINH-SANG VAN NGUYEN was born in Bentre, Vietnam. He is currently pursuing the master's degree in wireless communications. He has worked closely with Dr. Thuan with the Wireless Communications and Signal Processing Research Group, Industrial University of Ho Chi Minh City, Vietnam. His research interests include electronic design, signal processing in wireless communications networks, non-orthogonal multiple access, and physical layer security.

ANH-TU LE was born in Lam Dong, Vietnam. He is currently pursuing the master's degree in communication and information system in the field of wireless communications. He is currently a Research Assistant with the WICOM Laboratory, which was led by Dr. Thuan. He has authored or coauthored over five technical articles published in peer-reviewed international journals. His research interests include the wireless channel modeling, NOMA, cognitive radio, and MIMO.

KHALED M. RABIE (Senior Member, IEEE) received the B.S. degree (Hons.) from Tripoli University, Libya, in 2008, and the M.Sc. degree and the Ph.D. degree in electrical and electronic engineering from The University of Manchester, Manchester, U.K., in 2010 and 2015, respectively.

He joined the Manchester Metropolitan University (MMU), U.K., where he is currently an Assistant Professor with the Department of Engineering. He has published more than 90 articles in prestigious journals and international conferences. His primary research interest includes various aspects of the next-generation wireless communication systems. He is also a Fellow of the U.K. Higher Education Academy (FHEA). He has received numerous awards over the past few years in recognition of his research contributions, including the Best Student Paper Award at the IEEE ISPLC, TX, USA, in 2015, the MMU Outstanding Knowledge Exchange Project Award of 2016, and the IEEE Access Editor of the Month Award for August 2019. He serves regularly on the Technical Program Committee of several major IEEE conferences, such as GLOBECOM, ICC, VTC, and so on. He currently serves as an Associate Editor for IEEE Access, an Area Editor for *Physical Communication* (Elsevier), and an Executive Editor for the *Transactions on Emerging Telecommunications Technologies* (Wiley).

JIAYI ZHANG (Member, IEEE) received the B.Sc. and Ph.D. degrees in communication engineering from Beijing Jiaotong University, China, in 2007 and 2014, respectively.

From 2012 to 2013, he was a visiting Ph.D. student with the Wireless Group, University of Southampton, U.K. From 2014 to 2015, he was a Humboldt Research Fellow with the Institute for Digital Communications, University of Erlangen–Nuremberg, Germany. From 2014 to 2016, he was a Postdoctoral Research Associate with the Department of Electronic Engineering, Tsinghua University, China. Since 2016, he has been a Professor with the School of Electronic and Information Engineering, Beijing Jiaotong University. His current research interests include massive MIMO, large intelligent surface, communication theory, and applied mathematics. He was recognized as an Exemplary Reviewer of the IEEE Communications Letters, in 2015 and 2016, and the IEEE Transactions on Communications, in 2017. He was the Lead Guest Editor of the Special Issue on Multiple Antenna Technologies for Beyond 5G of the IEEE Journal on Selected Areas in Communications. He currently serves as an Associate Editor for the IEEE Transactions on Communications, the IEEE Communications Letters, IEEE Access, and *IET Communications*.